

THE MAGNETIC FIELD OF THE SCREENED FLAT THREE-PHASE HIGH CURRENT BUSDUCT

PH.D., D.SC., ENG. ZYGMUNT PIĄTEK, UNIV. PROF.

PH.D., ENG. DARIUSZ KUSIAK

M.SC., ENG. TOMASZ SZCZEGIELNIAK

Abstract: In the paper all components of total magnetic field in the screen and onto his internal and external surface as a function variables r and Θ of cylindrical coordinates were calculated. Total current density induced in the screen of flat high current busduct was taken into account. Total magnetic field of screen is defined according to the reverse reaction between eddy currents and this field is an elliptical, rotating field.

Key words: High current busduct, tubular busbar, magnetic field, eddy currents

INTRODUCTION

One of the structural solutions for the construction of high current busducts is provided in the shape of the so-called flat three-pole high current busduct [1-2] – fig. 1.

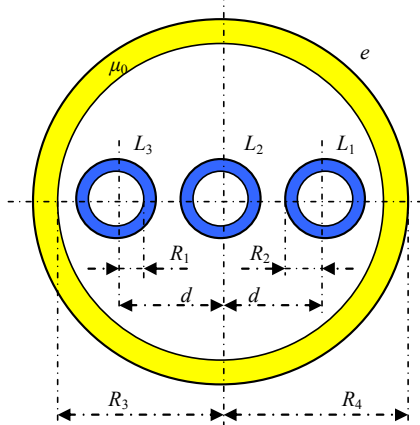


Fig. 1. Flat three-pole high current busduct

Screened three-phase high current busducts are applied as reliable and safe large-current connectors (up to 9 kA) within the range of medium and high voltages (up to 275 kV) [3-7].

Due to large rated currents the intensity values of the variable magnetic fields generated by such insulated busducts are high even at nominal rating conditions. Those fields, having power frequency, exert influence on their own components and on the broadly understood environment - other devices and electric power units, steel structures, electronic data control, monitoring and transmission circuitry, the natural environment and on man.

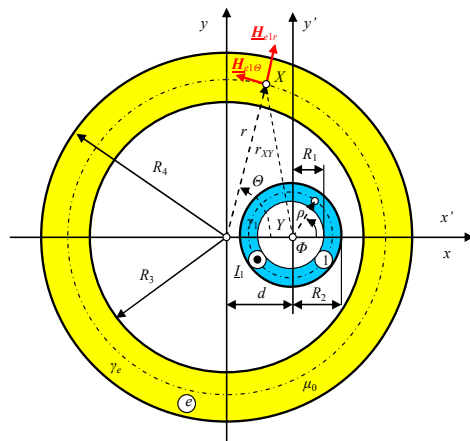


Fig. 2. Tubular screen with an internal non-coaxial tubular conductor

By exceeding certain permissible intensities those fields can lead to an irregular operation of electrical appliances, an overheating of steel constructions and deterioration of the natural environment. They can also be hazardous to humans [8]. All these problems can be traced to the issue of electromagnetic compatibility which requires a precise determination of intensity values for power frequency magnetic fields in various structural solutions for the construction of high current busducts.

The magnetic field of a three-phase system is the superposition of the fields generated by the phase conductor currents or, in general, of the fields in a non-coaxial system – fig. 2.

In the case of single-core cables and single-pole high current busducts the phase conductor and the screen constitute a coaxial system. In this situation the magnetic field inside and outside the screen does not depend on the screen presence - the tubular shield for the magnetic field of the particular own bus bar is an open, anomalous screen. A different situation prevails in the case of a non-coaxial phase conductor and screen, as in multi-core and multi-pole current busducts. In the above case the magnetic field inside and outside the conducting pipe screen depends on its presence, which shall be demonstrated in the present article. To be precise, we shall examine the magnetic field of a system consisting of a tubular screen and a tubular non-coaxial phase conductor (fig. 2). The analysis of the influence exerted by the conducting screen on the magnetic field distribution shall be restricted to an examination of this field in the screen and on its internal and external surfaces.

1 THE PHASE CURRENT MAGNETIC FIELD

The vectorial magnetic potential generated by the current I_1 (fig. 2) has only one component along the Oz axis and is a potential generated by an external source in relation to the conducting screen and according to its definition, in a cylindrical co-ordinate system (ρ, Φ, z) connected with another conductor, we obtain

$$\underline{A}^w(r_{XY}) = \frac{\mu_0 I_1}{2\pi} \ln \frac{1}{r_{XY}} + \underline{A}_0 \quad (1)$$

where the \underline{A}_0 constant can be adopted arbitrarily.

The above vectorial magnetic potential can be expressed with a local cylindrical coordinate system (r, θ, z) , i.e.

$\underline{A}^w(r, \theta) = \mathbf{1}_z \underline{A}^w(r, \theta)$. Next, after expanding the $\ln \frac{1}{r_{XY}}$ expression into the Fourier series, at the point $X(r, \theta)$, the one for which $r > d$, the vectorial magnetic potential has the following form [1, 2, 9, 10]

$$\underline{A}^w(r, \theta) = \frac{\mu_0 I_1}{2\pi} \left[\ln \frac{1}{r} + \sum_{n=1}^{\infty} \frac{1}{n} \left(\frac{d}{r} \right)^n \cos n\theta \right] + \underline{A}_0 \quad (2)$$

We shall determine the magnetic field intensity vector using the vectorial magnetic potential definition in order to obtain

$$\underline{H}^w(r, \theta) = \mathbf{1}_r \underline{H}_r^w(r, \theta) + \mathbf{1}_\theta \underline{H}_\theta^w(r, \theta) \quad (3)$$

where

$$\underline{H}_r^w(r, \theta) = -\frac{I_1}{2\pi r} \sum_{n=0}^{\infty} \left(\frac{d}{r} \right)^n \sin n\theta$$

and

$$\underline{H}_\theta^w(r, \theta) = \frac{I_1}{2\pi r} \sum_{n=0}^{\infty} \left(\frac{d}{r} \right)^n \cos n\theta$$

The \underline{H}^w magnetic field is a field generated by an external source in relation to the screen; therefore it is present in the screen, as well as on its internal and external surfaces. Its modulus is expressed with the following formula

$$H^w(r, \theta) = \sqrt{[H_r^w(r, \theta)]^2 + [H_\theta^w(r, \theta)]^2} \quad (4)$$

2 THE MAGNETIC FIELD IN THE SCREEN OF A SINGLE-CORE SYSTEM

The phase conductor magnetic field induces eddy currents in the screen – the so-called internal proximity effect takes place – fig. 3.

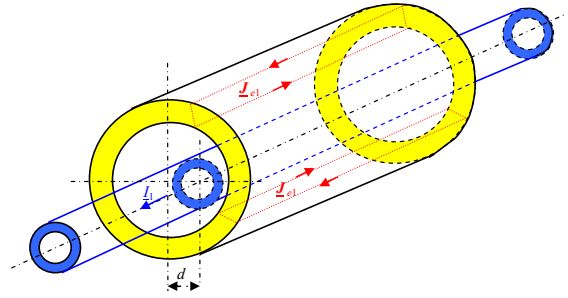


Fig. 3. Eddy currents induced in the screen

The currents generate a magnetic field of reflexive interaction. The resultant magnetic field on the internal and external screen surfaces is the vectorial sum of the appropriate reflexive interaction field and the field generated by the current in the phase conductor. If we restrict our analysis to an examination of the influence exerted by the conducting screen on the magnetic field distribution only on the internal and external surfaces of the screen, we can take advantage of the solution presented in the papers [9, 10] in which the density of the current induced in the screen is expressed with the following formula

$$\underline{J}_{e1}(r, \theta) = \underline{J}_{e10}(r) + \sum_{n=1}^{\infty} \underline{J}_{e1n}(r, \theta) \quad (5)$$

where

$$\underline{J}_{e10}(r) = \frac{\Gamma_e I_1}{2\pi R_3} \frac{b_0 I_0(\Gamma_e r) + c_0 K_0(\Gamma_e r)}{d_0}$$

and

$$\underline{J}_{e1n}(r, \theta) = \frac{\Gamma_e I_1}{\pi R_3} \underline{g}_n(r) \cos n\theta$$

In the above formulas the complex propagation constant of the electromagnetic wave in the conducting screen is

expressed with the following equation $\underline{\Gamma}_e = \sqrt{j\omega\mu_0\gamma_e}$, where ω denotes the phase current ripple, $\mu_0 = 4\pi 10^{-7} \text{ H} \cdot \text{m}^{-1}$ the magnetic permeability of free space and γ_e is the screen conductivity. The functions $I_0(\underline{\Gamma}_e r)$ and $K_0(\underline{\Gamma}_e r)$ are the modified Bessel functions of respectively the first and second kind in the zero order. The constant data are expressed with the following formulas:

$$\underline{d}_0 = I_1(\underline{\Gamma}_e R_4) K_1(\underline{\Gamma}_e R_3) - I_1(\underline{\Gamma}_e R_3) K_1(\underline{\Gamma}_e R_4)$$

$$\underline{b}_0 = \beta K_1(\underline{\Gamma}_e R_3) - K_1(\underline{\Gamma}_e R_4)$$

and

$$\underline{c}_0 = \beta I_1(\underline{\Gamma}_e R_3) - I_1(\underline{\Gamma}_e R_4)$$

while $\beta = \frac{R_3}{R_4}$, ($0 \leq \beta \leq 1$). The function

$$\underline{g}_n(r) = -\left(\frac{d}{R_3}\right)^n \times \frac{K_{n-1}(\underline{\Gamma}_e R_4) I_n(\underline{\Gamma}_e r) + I_{n-1}(\underline{\Gamma}_e R_4) K_n(\underline{\Gamma}_e r)}{d_n}$$

where

$$\underline{d}_n = I_{n-1}(\underline{\Gamma}_e R_4) K_{n+1}(\underline{\Gamma}_e R_3) - I_{n+1}(\underline{\Gamma}_e R_3) K_{n-1}(\underline{\Gamma}_e R_4)$$

The function $I_n(\underline{\Gamma}_e r)$, $K_n(\underline{\Gamma}_e r)$, $I_{n-1}(\underline{\Gamma}_e R_4)$, $K_{n+1}(\underline{\Gamma}_e R_3)$, $I_{n+1}(\underline{\Gamma}_e R_3)$ and $K_{n-1}(\underline{\Gamma}_e R_4)$ which appear in the above formulas are the modified Bessel functions of respectively the first and second kind in the n th, $n-1$ and $n+1$ orders.

Next, from the second Maxwell equation

$\underline{H}_{e1}(r, \Theta) = -\frac{1}{\underline{\Gamma}_e^2} \text{rot} \underline{J}_{e1}(r, \Theta)$ we obtain¹ the magnetic field in the screen under analysis ($R_3 \leq r \leq R_4$)

$$\underline{H}_{e1}(r, \Theta) = \mathbf{1}_r \underline{H}_{e1r}(r, \Theta) + \mathbf{1}_\Theta \underline{H}_{e1\Theta}(r, \Theta) \quad (6)$$

where the radial component

$$\underline{H}_{e1r}(r, \Theta) = \frac{I_1}{\pi R_3} \frac{1}{\underline{\Gamma}_e r} \sum_{n=1}^{\infty} n \underline{g}_n(r) \sin n\Theta$$

¹ From the paper [11] using the formula (167) on page 281 for $n=1$ we derive $I_{-1}(\underline{\Gamma}r) = I_1(\underline{\Gamma}r)$ and using the formula (212) on page 285 we derive $K_{-1}(\underline{\Gamma}r) = K_1(\underline{\Gamma}r)$. From the formulas (165) and (173) on page 281 we derive $\frac{dI_n(\underline{\Gamma}r)}{dr} = -\frac{n}{r} I_n(\underline{\Gamma}r) + \underline{\Gamma} I_{n-1}(\underline{\Gamma}r)$ and on the basis of the formula (167) on page 281 we also obtain $2nI_n(\underline{\Gamma}r) = \underline{\Gamma}r I_{n-1}(\underline{\Gamma}r) - \underline{\Gamma}r I_{n+1}(\underline{\Gamma}r)$. From the formulas (210) and (218) on page 285 we derive $\frac{dK_n(\underline{\Gamma}r)}{dr} = -\frac{n}{r} K_n(\underline{\Gamma}r) - \underline{\Gamma} K_{n-1}(\underline{\Gamma}r)$ and on the basis of the formula (210) on page 281 we also obtain $2nK_n(\underline{\Gamma}r) = \underline{\Gamma}r K_{n+1}(\underline{\Gamma}r) - \underline{\Gamma}r K_{n-1}(\underline{\Gamma}r)$.

The tangent component is expressed by the sum of those components $n=0$ and $n \geq 1$, i.e.

$$\underline{H}_{e1\Theta}(r, \Theta) = \underline{H}_{e1\Theta 0}(r) + \sum_{n=1}^{\infty} \underline{H}_{e1\Theta n}(r, \Theta) \quad (7)$$

The first addend ($n=0$)

$$\underline{H}_{e1\Theta 0}(r) = \frac{I_1}{2\pi R_3} \frac{\underline{b}_0 I_1(\underline{\Gamma}_e r) - \underline{c}_0 K_1(\underline{\Gamma}_e r)}{\underline{d}_0}$$

For the second addend ($n \geq 1$)

$$\underline{H}_{e1\Theta n}(r, \Theta) = \frac{I_1}{\pi R_3} \frac{1}{\underline{\Gamma}_e r} f_{-n}(r) \cos n\Theta$$

where the function

$$f_{-n}(r) = \left(\frac{d}{R_3}\right) \frac{1}{\underline{d}_n} \left\{ K_{n-1}(\underline{\Gamma}_e R_4) [n I_n(\underline{\Gamma}_e r) - \underline{\Gamma}_e r I_{n-1}(\underline{\Gamma}_e r)] + I_{n-1}(\underline{\Gamma}_e R_4) [n K_n(\underline{\Gamma}_e r) + \underline{\Gamma}_e r K_{n-1}(\underline{\Gamma}_e r)] \right\}$$

If a phase conductor is placed on the left of the screen axis, the magnetic field in all the areas is expressed with the above formulas supplemented with the $(-1)^n$ factor. It enables magnetic field analysis of screened single-phase systems, as well as three-phase flat and symmetric ones.

3 THE ELLIPTIC MAGNETIC FIELD

The amplitudes of the intensity components of the magnetic field in the screen are not identical, while the components also have different initial phases, i.e. $H_{e1r}(r, \Theta) \neq H_{e1\Theta}(r, \Theta)$ and $\varphi_{e1r}(r, \Theta) \neq \varphi_{e1\Theta}(r, \Theta)$.

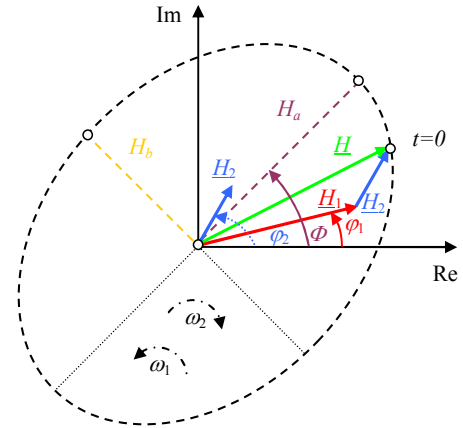


Fig. 4. The elliptic magnetic field

In that case, along with the change in time, during one period T , the end of the resultant vector, in function of the phase shift $\varphi = \varphi_{e1\Theta} - \varphi_{e1r}$ of the vector components, traces a straight line or ellipsis whose semi-major axis value H_a (fig. 4), the field modulus, does not equal the root of the squares of the magnetic field component amplitudes. We can then derive [8], denoting the semi-major axis quantity as

$$H_a(r, \Theta) = \max_{t \in (0, T)} H(r, \Theta, t) = H_1(r, \Theta) + H_2(r, \Theta) \quad (8)$$

where

$$\underline{H}_1(r, \Theta) = \frac{1}{2} [\underline{H}_{e1r}(r, \Theta) + j \underline{H}_{e1\theta}(r, \Theta)] = H_1 \exp[j\varphi_1(r, \Theta)]$$

and

$$\underline{H}_2(r, \Theta) = \frac{1}{2} [\underline{H}_{e2r}^*(r, \Theta) + j \underline{H}_{e2\theta}^*(r, \Theta)] = H_2 \exp[j\varphi_2(r, \Theta)]$$

4 THE MAGNETIC FIELD IN THE SCREEN OF A FLAT THREE-PHASE SYSTEM

The magnetic field in the screen ($R_3 \leq r \leq R_4$) is defined with the following formula

$$\underline{H}_e(r, \Theta) = \underline{H}_{e1}(r, \Theta) + \underline{H}_{e2}(r, \Theta) + \underline{H}_{e3}(r, \Theta) \quad (9)$$

The $\underline{H}_{e1}(r, \Theta)$ magnetic field is expressed with the formula (6). The $\underline{H}_{e2}(r, \Theta)$ magnetic field has only one tangent component

$$\underline{H}_{e2\theta}(r) = \frac{I_2}{2\pi R_3} \frac{b_0 I_1(\underline{\Gamma}_2 r) - c_0 K_1(\underline{\Gamma}_2 r)}{d_0} \quad (10)$$

The $\underline{H}_{e3}(r, \Theta)$ magnetic field components are expressed as

$$\underline{H}_{e3r}(r, \Theta) = \frac{I_3}{\pi R_3} \frac{1}{\underline{\Gamma}_2 r} \sum_{n=1}^{\infty} (-1)^n n \underline{g}_n(r) \sin n\Theta \quad (11)$$

and

$$\underline{H}_{e3\theta}(r, \Theta) = \underline{H}_{e3\theta 0}(r) + \sum_{n=1}^{\infty} \underline{H}_{e3\theta n}(r, \Theta) \quad (11a)$$

where for $n=0$

$$\underline{H}_{e3\theta 0}(r) = \frac{I_3}{2\pi R_3} \frac{b_0 I_1(\underline{\Gamma}_2 r) - c_0 K_1(\underline{\Gamma}_2 r)}{d_0} \quad (11b)$$

and for $n \geq 1$

$$\underline{H}_{e3\theta n}(r, \Theta) = \frac{I_3}{\pi R_3} \frac{1}{\underline{\Gamma}_2 r} (-1)^n \underline{f}_n(r) \cos n\Theta \quad (11c)$$

If the phase currents are symmetric, i.e.

$$\underline{I}_2 = \exp[-j\frac{2}{3}\pi] \underline{I}_1 \quad \text{oraz} \quad \underline{I}_3 = \exp[j\frac{2}{3}\pi] \underline{I}_1 \quad (12)$$

the total magnetic field in the screen of the flat three-phase high current busduct can be compared with the following field

$$\underline{H}_0 = \frac{I_1}{2\pi R_4} \quad (13)$$

We then derive formulas to obtain the relative components of the total magnetic field in the screen ($R_3 \leq r \leq R_4$ or $\beta \leq \xi \leq 1$) in the following forms:

$$\underline{h}_{er}(\xi, \Theta) = \frac{2}{\sqrt{2j\alpha\beta\xi}} \sum_{n=1}^{\infty} [(-1)^n + \exp(j\frac{2}{3}\pi)] n \underline{g}_n(\xi) \sin n\Theta \quad (14)$$

and

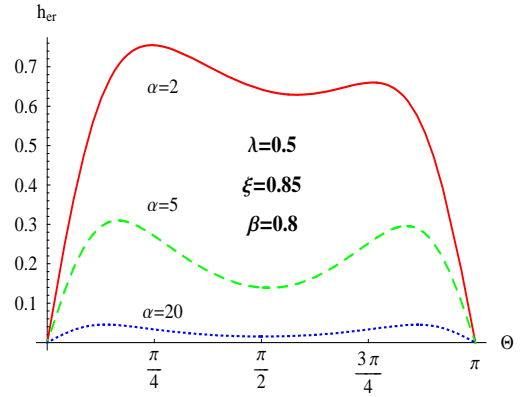
$$\underline{h}_{e\theta}(\xi, \Theta) = \frac{2}{\sqrt{2j\alpha\beta\xi}} \sum_{n=1}^{\infty} [(-1)^n + \exp(j\frac{2}{3}\pi)] \underline{f}_n(\xi) \cos n\Theta \quad (14a)$$

In these formulas the relative distance between the conductors $\lambda = \frac{d}{R_3}$ ($0 \leq \lambda < 1$), the relative variable

$\xi = \frac{r}{R_4}$ and the parameter $\beta = \frac{R_3}{R_4}$ where ($0 \leq \beta \leq 1$)

and $\alpha = \sqrt{\frac{\omega\mu_0\gamma_e}{2}} R_4$. The distribution of these components is depicted in figures 5 and 6.

a)



b)

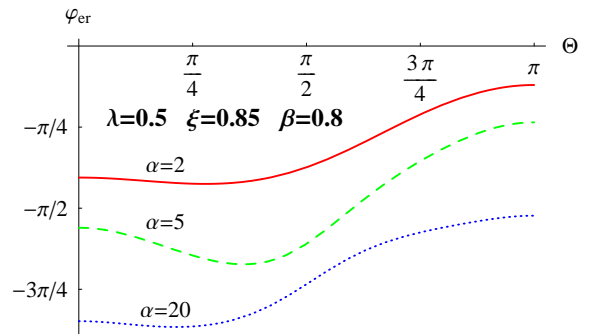
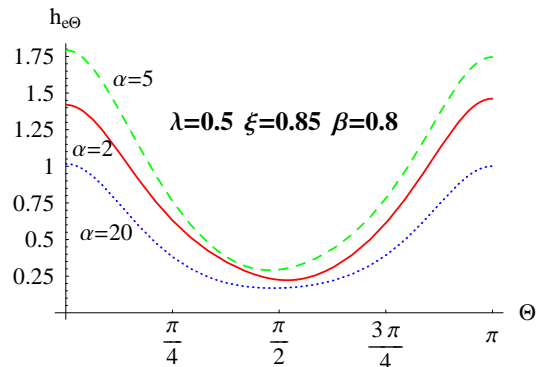


Fig. 5. The radial component distribution for the total magnetic field in the screen of the flat three-phase high current busduct: a) the modulus, b) the argument

a)



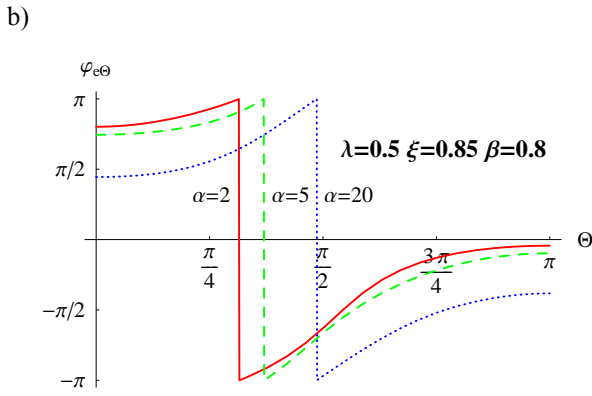


Fig. 6. The tangent component distribution for the total magnetic field in the screen of the flat three-phase high current busduct: a) the modulus, b) the argument

The $\underline{H}_e(r, \Theta)$ field component arguments are functions of the variables ξ and Θ , which means the field is an ellipsis whose semi-major axis value is expressed with the formula (8a). The distribution of this quantity in the screen for various values of the parameter α in the angle function Θ is depicted in figure 7.

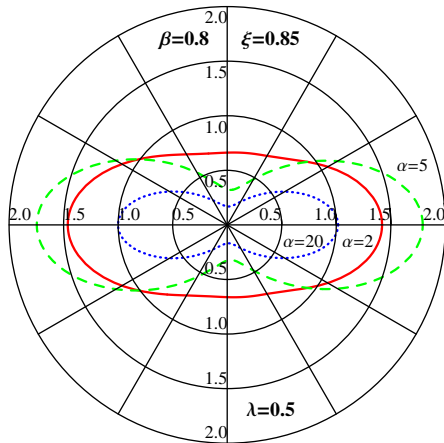


Fig. 7. The distribution of the relative modulus quantity of the total magnetic field in the screen of the flat three-phase high current busduct

If we assume $\xi = \beta$ in the formulas derived above, we obtain the magnetic field on the internal surface of the screen – fig. 8, 9 and 10.

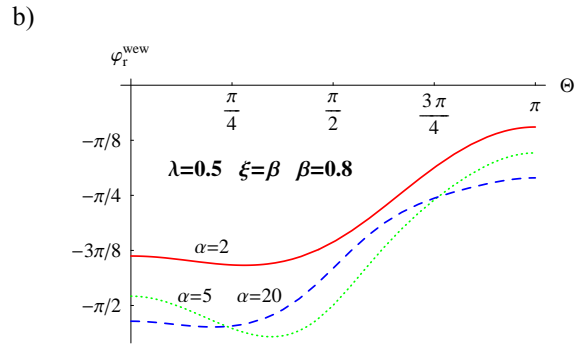
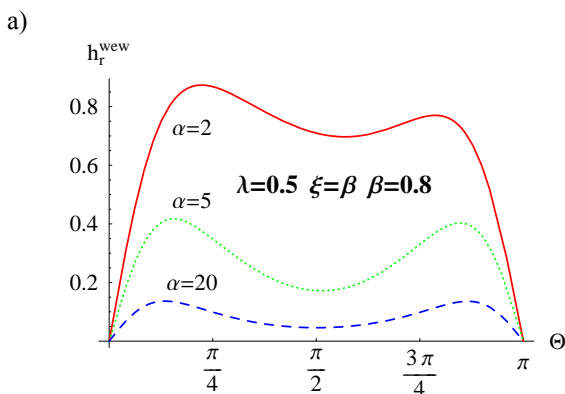


Fig. 8. The distribution of the radial component of the total magnetic field on the internal screen surface: a) the modulus, b) the argument

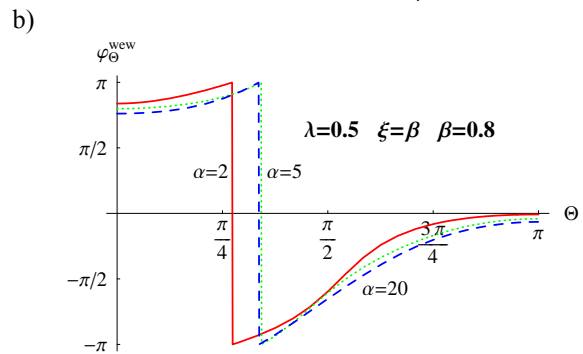
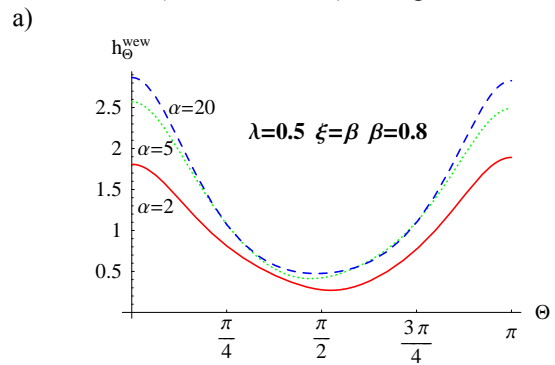


Fig. 9. The distribution of the tangent component of the total magnetic field on the internal screen surface: a) the modulus, b) the argument

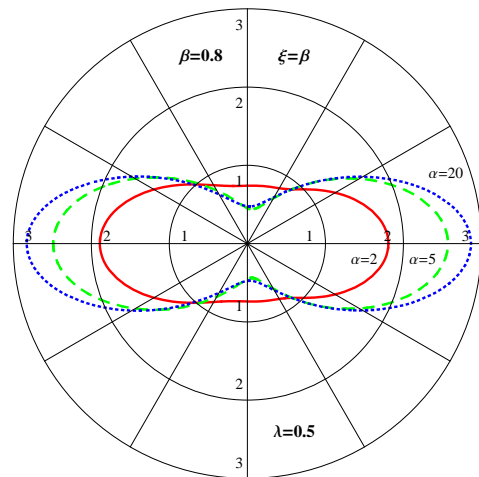


Fig. 10. The distribution of the total magnetic field modulus for the internal screen surface

In a similar manner, assuming $\xi = 1$, we obtain the magnetic field on external surface of the screen – fig. 11, 12 and 13.

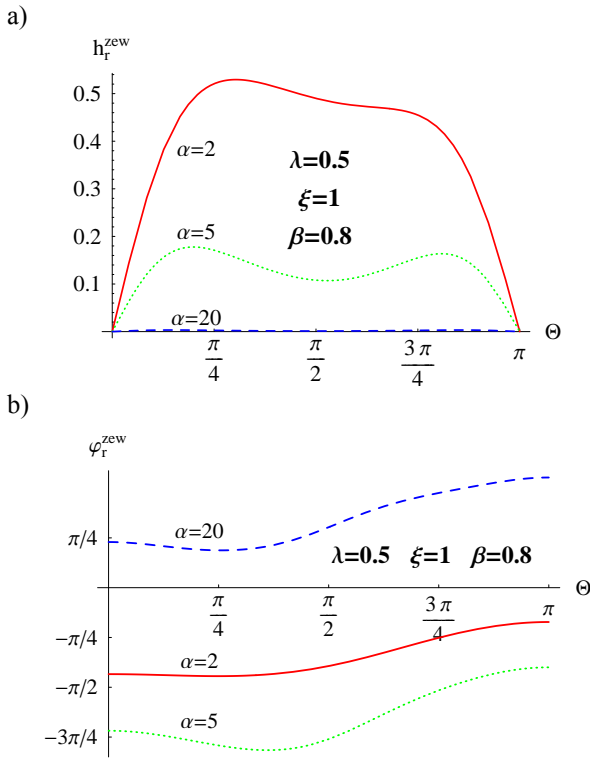


Fig. 11. The distribution of the radial component of the total magnetic field on the external screen surface: a) the modulus, b) the argument

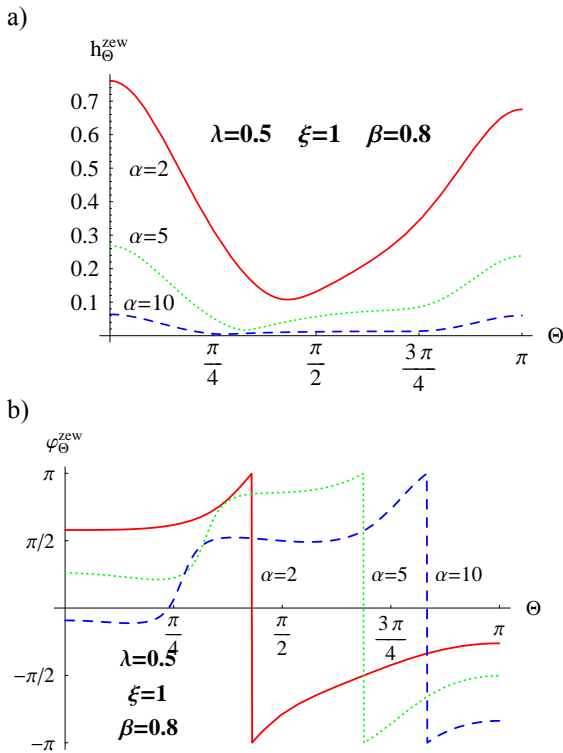


Fig. 12. The distribution of the tangent component of the total magnetic field on the external screen surface: a) the modulus, b) the argument

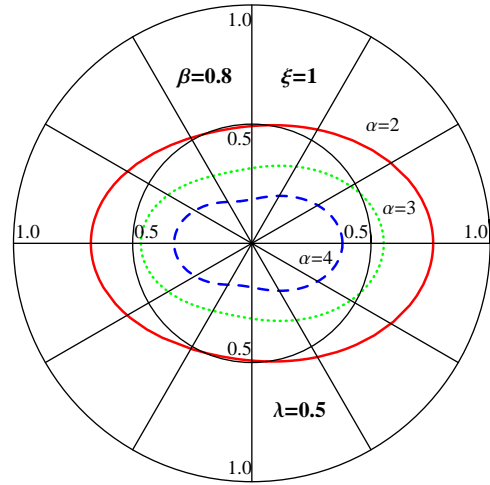


Fig. 13. The distribution the total magnetic field modulus for the external screen surface

5 CONCLUSIONS

From the above figures it follows that the magnetic field intensity in the screen and on its internal and external surfaces assumes the highest values at points lying in the closest proximity to the phase conductors. Despite the current symmetry the magnetic field intensity distribution is asymmetric. The field is a harmonious, rotating field.

The magnitude of the magnetic field changes depends on the coefficients λ and α , i.e. on the screen conductivity and crosswise dimensions and the current frequency in the phase conductors. With the rise of the parameter α the intensity value of the magnetic field on the internal screen surface grows, while in the screen itself we observe a certain reduction in this field. However, on the external surface this reduction is significant. It is the result of the reflexive interaction of eddy currents induced in the screen. Such a screen is no longer the so-called open, anomalous screen – the field in the external area depends on the screen presence.

As regards already implemented high current busducts, at industrial frequency, the α parameter value is within the range of 10 to 20. Within this range, as demonstrated in figures 7, 10 i 13, the magnetic field changes in the screen, on its internal surface and, in particular, on its external surface are significant. Hence the conclusion that an analysis of the magnetic field of the screened busduct in question should allow for the presence of a conducting screen also in the case of power frequency.

6 REFERENCES

- [1] Piątek Z.: Modeling of lines, cables and high-current busducts (in Polish). Wyd. Pol. Częst., Częstochowa 2007.
- [2] Piątek Z.: Impedances of Tubular High Current Busducts. Series Progress in High-Voltage technique, Vol. 28, Polish Academy of Sciences, Committee of Electrical Engineering, Wyd. Pol. Częst., Częstochowa 2008.

- [3] Okamura K., Ishiyama F., Kawamura T.: Characteristics of Power Frequency Field in Three Phase Enclosure Type GIL Model. High Voltage Engineering Symposium, 22-27 August 1999, Conference Publication No. 467, © IEE, 1999.
- [4] Rajaraman R., Satyanarayana S., Bhoomaiah A., Jain H.S.: A new optimised design of integrated three phase gas insulated busduct. High Voltage Engineering, 1999. Eleventh International Symposium on (Conf. Publ. No. 467), Volume 5, Issue , 1999, pp. 414 - 417 vol.5.
- [5] Guillen M., Bertrand M.: Optimized gas insulated transmission line (in French). Revue de l'Electricité et de l'Electronique (REE) (5) (May 2000) pp. 58-64.
- [6] Guillen M., Buret F., Béréal A.: Lightning impulse withstand of a gas-insulated line filled N₂-SF₆. 11 ISH, paper 3.71.S18, London, 23-27 August 1999.
- [7] Guillen M., Girodet A., Thuries E.: Three-Phase Gas-Insulated Transmission Line. Conf. Proc. POWER DELIVERY '97, June 17-19, 1997, Madrid, Spain, pp. 396-409.
- [8] Piątek Z.: Magnetic field in high-current isolated-phase enclosed bus ducts surroundings (in Polish). Zesz. Nauk. Pol. Śl. 1999, Elektryka, z. 166.
- [9] Piątek Z.: Eddy Currents Induced in the Screen of a Non-Coaxial Cable. Przegląd Elektrotechniczny - Konferencje, ISSN 1731-6106, R. 5, Nr 2/2007, pp. 29-32.
- [10] Piątek Z.: Eddy currents in the screen of a three-phase symmetrical transmission line (in Polish). Wiadomości Elektrotechniczne, Year LXXV, No 3, 2008, pp. 17-21.
- [11] Mc Lachlan N.W.: Bessel functions for engineers (in Polish). PWN, Warsaw 1964.

Authors:

Ph.D., D.Sc., Eng., Univ. Prof. Zygmunt Piątek, Czestochowa University of Technology, Faculty of Environmental Engineering and Protection Institute of Environmental Engineering, ul. Brzeźnicka 60a, 42-200 Częstochowa, E-mail: zygmunt.piatek@interia.pl

Ph.D., Eng. Dariusz Kusiak, Czestochowa University of Technology, Faculty of Electrical Engineering, Institute of Industrial Electrotechnics, Aleja Armii Krajowej 17, 42-200 Częstochowa, E-mail: dariuszkusiak@wp.pl

M.Sc., Eng. Tomasz Szczegielniak, Czestochowa University of Technology, Faculty of Environmental Engineering and Protection, Doctorate Study, ul. Dąbrowskiego 73, 42-200 Częstochowa, E-mail: szczegielniakt@interia.pl